Preheat Effects on Shock Propagation in Indirect-Drive Inertial Confinement Fusion Ablator Materials

R. E. Olson,[1] R. J. Leeper,[1] A. Nobile,[2] and J. A. Oertel[2]
[1]*Sandia National Laboratories, Albuquerque, New Mexico 87185, USA*
[2]*Los Alamos National Laboratory, Los Alamos, New Mexico 87545, USA*
(Received 14 April 2003; published 3 December 2003)

The velocities and temperatures of shock waves generated by laser-driven hohlraum radiation fields have been measured for several indirect-drive inertial confinement fusion capsule ablator materials. For the first time, a time-resolved measurement of the preheat temperature ahead of the shock front has been performed and included in the analysis. It is found that preheat ahead of the shock front can cause significant shock propagation variations in the ignition capsule ablator materials being considered for the National Ignition Facility (NIF). If unaccounted for, these preheat effects could potentially preclude ignition at the NIF.

DOI: 10.1103/PhysRevLett.91.235002 PACS numbers: 52.57.–z, 52.35.Tc

Thermonuclear ignition via indirect-drive inertial confinement fusion (ICF) is one of the primary goals of the National Ignition Facility (NIF) [1] in the U.S. and of the Laser Megajoule (LMJ) [2] in France. In the indirect-drive ICF option, the high power input (~500 TW) of 0.35 μm laser beams will be absorbed in a high-Z enclosure (or "hohlraum") that surrounds a low-Z spherical shell (or "capsule") containing a layer of solid cryogenic deuterium-tritium (DT) fuel. The hohlraum walls are heated via a carefully controlled sequence of laser pulses. The soft x rays emitted by the hohlraum walls freely traverse the region between the capsule and the wall and are strongly absorbed by the capsule, rapidly ablating the low-Z material and setting up a sequence of shock waves within the capsule. A precise understanding of the x-ray ablation and shock propagation process will be critical to the proper implosion sequence and to the achievement of indirect-drive ICF ignition. For example, ignition capsule sensitivity calculations indicate that timing of the shock sequence must be predicted and measured to within ~100 ps [3,4].

The time-dependent magnitude of the x-ray flux upon the indirect-drive capsule is usually described in terms of a radiation temperature history having an ~80–90 eV, ~10 ns foot pulse followed by a sequence of hohlraum temperature increases that rise to a peak of ~300 eV within the next ~8 ns [5,6]. In this manner, the required shock sequence is set up within the imploding capsule. It is important to note, however, that the concept of a hohlraum radiation temperature provides only an approximate description of the hohlraum x-ray flux. In reality, the x-ray flux absorbed by the capsule is a combination of soft x rays emitted by the high-Z hohlraum walls (which are approximately blackbody in spectrum) along with the higher energy x rays (such as Au m-band x rays) that originate in and near the hot (~1–5 keV), low density ($n_e < 10^{22}$ cm^{-3}) coronal plasma in which the 0.35 μm laser light is absorbed and converted into x rays. The high-energy photons originating in and near this hohlraum x-ray source plasma can penetrate beyond the capsule ablation surface and preheat material ahead of the shock front. Although this preheat has been seen in previous indirect-drive ablator experiments [7], in this Letter we describe the first time-resolved measurements of indirect-drive ablator preheat temperature and its effects upon shock propagation. Results of sensitivity calculations are used to demonstrate that the ablator preheat effects of this magnitude can significantly alter ignition capsule shock timing and must be accurately included in the capsule design calculations and measurement techniques used in the NIF ignition program.

In the U.S. ICF program, there are presently three materials being considered as candidates for an indirect-drive ignition capsule — beryllium with 0.9% copper ($Be_{991}Cu_9$) [6,8], polyimide ($C_{22}H_{11}N_2O_5$) [9,10], and CH with 5% oxygen and ~0.25%–0.45% germanium [11]. Of these materials, beryllium has the advantages of lowest opacity, highest density, lowest specific heat, highest tensile strength, and highest thermal conductivity [12]. Although beryllium is emphasized here, comparable details for Ge-doped CH and polyimide are provided elsewhere [13].

The experiments were conducted at the University of Rochester's 30 kJ, 0.35 μm Omega laser [14] and employed 15 of the 60 Omega laser beams as a drive to produce hohlraum radiation fields in the range of 120–200 eV. The hohlraums had 25 μm thick gold walls and were 1.6 mm in diameter and 1.2 mm long, with one laser entrance hole (LEH). The ablator samples were 0.85 mm in diameter and were mounted over a 0.80 mm diameter hole on the side opposite the LEH. The primary diagnostic was a streaked optical pyrometer (SOP) [15] [an optical telescope, focusing mirrors, filters, imaging slit, streak camera, charge-coupled device (CCD) camera, and optical fiducial system] filtered to view the emission of ~300 nm UV light emitted as the shock arrives at the

exterior surface of the sample. X-ray diagnostics viewing the interior of the hohlraum through the LEH included x-ray framing cameras [16], filtered photocathode x-ray detectors ("Dante" XRDs) [17], and photoconductive detectors [18]. These x-ray diagnostics are used to confirm the time-, spatially, and spectrally dependent x-ray emission from the hohlraum walls and from the x-ray driven side of the ablator samples.

Examples of SOP images from step- and wedge-shaped polyimide, $Be_{991}Cu_9$, and Ge-doped CH samples are shown in Fig. 1. Time increases from left to right, and the fiducials are at ~550 ps intervals. Prior to the experiments, the thickness of each $Be_{991}Cu_9$ sample as a function of position across its entire surface was recorded with submicron precision via a dual active confocal laser contouring measurement [19]. With detailed thickness information, the step images provide a measurement of shock velocity averaged over the breakout time interval, and the wedge images provide a time-resolved measurement of shock velocity [7,15,20]. The fiducials in the present experiments were time tied to the laser pulse via separate laser shots in which the SOP viewed a laser-produced plasma positioned at the target chamber center. Using this time tie, lineouts through the streaked images such as those shown in Fig. 1 provide a measure of intensity vs time for the UV emission from the surface of the ablator sample. The intensity was calibrated using separate hohlraum experiments in which the UV emission from an aluminum step sample was viewed. Considering the aluminum equation of state to be a known standard, the measurement of emission from the aluminum step, together with the aluminum shock velocity determination and knowledge of the SOP filter set, provides a data unfold in terms of a temperature history at the exterior-facing surface of an ablator sample. A comparison of this measurement for a $Be_{991}Cu_9$ sample with calculations using the LASNEX radiation hydrodynamics code [21] is shown in Fig. 2. The data indicate that the cooler, exterior-facing surface of the 80 μm thick portion of the Be is gradually heated to a temperature of about 4 eV during the time prior to shock breakout. When the shock arrives at the exterior surface, the temperature jumps to about 15 eV. The dashed curve is the result of a LASNEX calculation for which the x-ray input is based upon the time-resolved Dante measurement of the interior of the ~160 eV hohlraum represented as an equivalent blackbody brightness temperature. For this brightness temperature treatment, only 1.6% of the peak flux is in photon energies above 1.5 keV (a spectrum that is, in fact, not consistent with our measurement indicating 5%–10% of the flux residing in the ~2.5 keV channel of the Dante instrument). As can be seen in the figure, the blackbody approximation of the hohlraum radiation field provides an incorrect calculation of the shock temperature and breakout time and entirely misses the radiation preheat features of the experiment. The solid curve is the result of a LASNEX calculation that uses an input in which the hohlraum radiation field has ~17% of the flux in photons with energies > 1.5 keV. This x-ray input for the calculation is the result of a fully integrated LASNEX calculation in which the measured on-target laser power is used as an input. This calculational method captures the main features of the measurement, including the preheat.

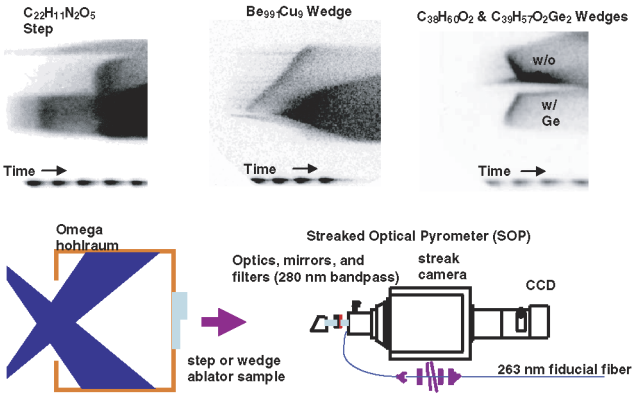

FIG. 1 (color online). Schematic of the hohlraum geometry and SOP with example data.

The Rankine-Hugoniot equations can be combined to relate the shock velocity D (km/s), pressure P (GPa), and specific volume V (cm^3/g) in the form [22]

$$D^2 = V_0^2(P - P_0)/(V_0 - V), \quad (1)$$

where subscripts indicate conditions ahead of the shock front. Equation (1) can be combined with a Be equation of state calculation [here we use a Sesame Be EOS (equation of state) table [23] based upon the model of Ref. [24]] to

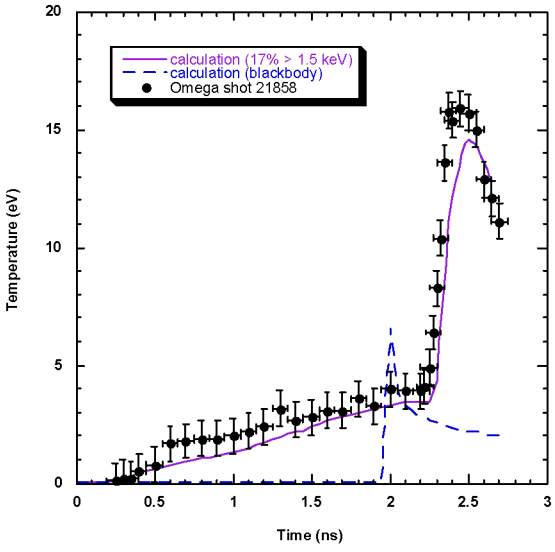

FIG. 2 (color online). Surface temperature of 80 μm $Be_{991}Cu_9$ step: data and simulations for an experiment done with an ~160 eV hohlraum.

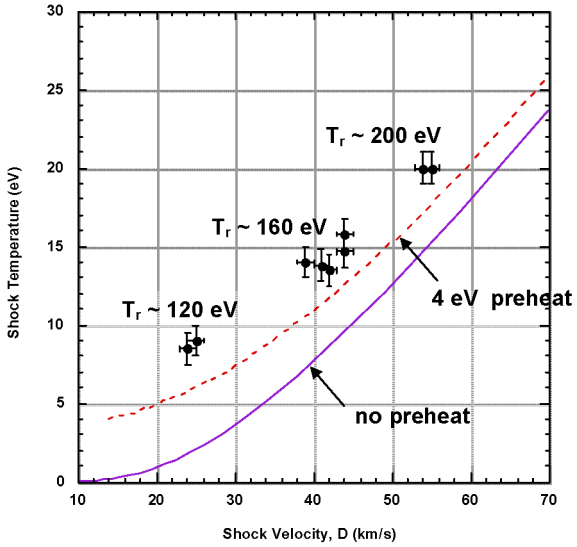

FIG. 3 (color online). Sesame shock Hugoniots with and without preheat compared to shock temperature and velocity measurements in experiments with hohlraum radiation field temperatures of 120, 160, and 200 eV.

give a predicted relationship between shock temperature and shock velocity as shown in Fig. 3. The data points are from Omega experiments using samples of the proposed $Be_{991}Cu_9$ indirect-drive ICF capsule material at hohlraum radiation temperatures ~120, 160, and 200 eV. The measurements are clearly not in agreement with the usual $P = 0$ single shock Hugoniot (solid curve in Fig. 3), but can be explained if an initial state preheated to > 4 eV is assumed (dashed curve).

Figure 4 illustrates some of the comparable measurements made in Ge-doped CH and polymide ablator samples. The SOP image shown in the upper right of Fig. 1 is from an experiment employing side-by-side wedges of Ge-doped (2% atomic) and undoped CH ablator samples. Intensity-time lineouts of these data (at approximately equivalent thickness positions) are shown in Fig. 4(a). These data clearly demonstrate that the Ge dopant can be used to decrease preheat and shock temperature in the CH ablator. The SOP image shown in the upper left of Fig. 1 is from an experiment using a polyimide step. An intensity-time lineout of these data (together with another lineout from a repeat of this experiment) is shown in Fig. 4(b). The SOP bandpass intensity prediction from a calculation (using the 17% $>$ 1.5 keV input spectrum) is also shown in the figure. This calculation completely misses the large preshock intensity signal of the polyimide experiments. At present, none of the preshock features seen in the polyimide experiments are understood, and future experiments to resolve this issue are being planned. We have also performed calculations exploring the sensitivities to opacity and equation of state (EOS) models and comparisons to data for all three ignition capsule ablator materials [13]. In all cases, it is found that these effects are less important than the spectral input preheat sensitivities.

The importance of ablator preheat can be illustrated via capsule design sensitivity calculations. One of the baseline NIF ignition capsule designs using the $Be_{991}Cu_9$ material is shown in Fig. 5 [6,12]. The hohlraum radiation drive for this capsule is shown in the usual manner as a plot of brightness temperature history. The total thermonuclear yields for four calculations are indicated in the figure. The drive flux in all four calculations follows the same brightness temperature history, but each calculation has a different spectra. At the end of the third shock (i.e., ~160 eV brightness temperature) the blackbody calculation has 1.6% of the flux in photons

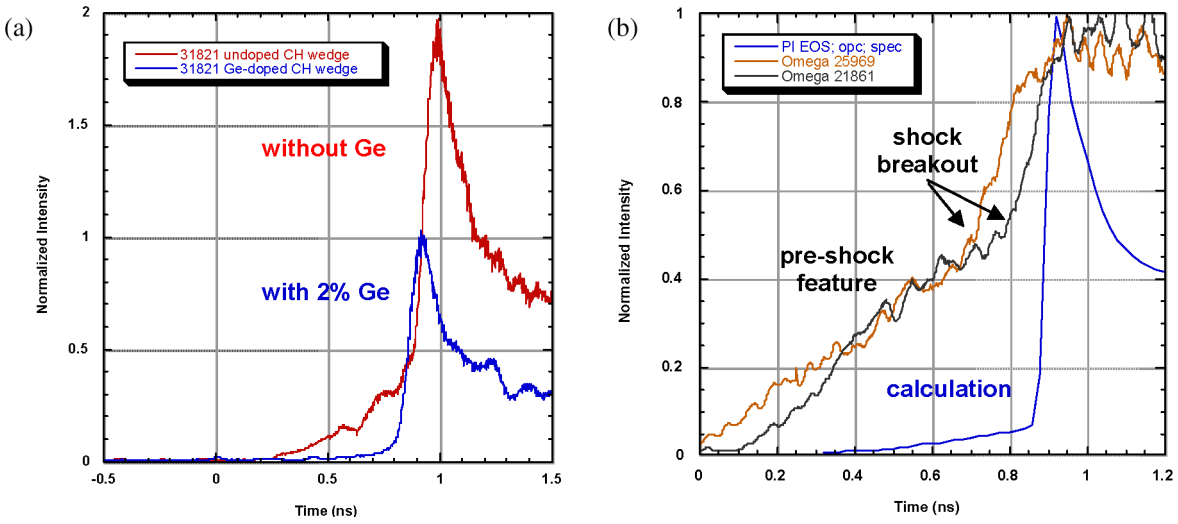

FIG. 4 (color online). (a) Comparison of shock and preheat intensities with and without Ge dopant (2% atomic) in a CH ablator. (b) A comparison of typical data with a calculation for preheat and shock intensities using a polyimide sample.

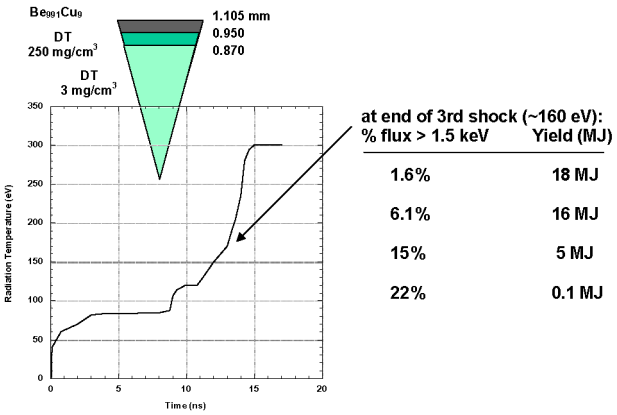

FIG. 5 (color online). An indirect-drive ICF capsule design [6,12] and results of design calculation variations on the spectral input.

with energy above 1.5 keV. The calculated yield is 18 MJ. In effect, this calculation does not include the effects of hot, laser-driven x-ray source plasma. At the same point in time, the second calculation has 6% of the flux in energies above 1.5 keV with the spectrum arranged such that the high-energy component is peaked at 2.5 keV (near the expected peak for Au *m*-band x rays). This is representative of a situation in which hohlraum wall albedo [20,25] is very high (i.e., $> 90\%$). The third and fourth calculations have a high-energy component of 15% and 22%, respectively. These would represent situations in which the hohlraum albedo is in agreement with the usual experimentally observed range (i.e., 80%–90%). It appears that the drop to below 1% design yield for this capsule design occurs with a drive spectrum having about 20% of its flux in photons with energies above 1.5 keV (i.e., a hohlraum albedo ~80%).

The thermonuclear yield sensitivity to flux spectrum is due primarily to changes in the shock timing. As described in Refs. [3,4], changes of ~100 ps in the timing of the first three shocks can result in significant yield degradation. Thus, it is not surprising that a 10%–20% change in shock velocity due to preheat ahead of the shock front might alter the timing of the shocks and thereby degrade the capsule yield. The Omega preheat measurements are consistent with a drive spectrum (at $Tr \sim 160$ eV) having approximately 17% of the flux in energies above 1.5 keV. This is consistent with a hohlraum wall albedo of about 80%–85%. An actual NIF or LMJ ignition capsule will be positioned in a larger scale hohlraum having a cryogenic He-H gas fill and, perhaps, an overall lower laser spot intensity. Also, in NIF the ignition target hohlraum wall might be a cocktail [25], instead of pure Au. Thus, the spectral details of the flux for an ignition capsule will be different from the Omega situation, but nonetheless must be accurately measured and included in the capsule design calculations. Providing this can be done, it is encouraging to note that it has been demonstrated in these experiments that ablator dopants can be used to alter (and, perhaps control) preheat and shock temperatures.

In summary, it is found that x-ray preheat ahead of an indirect-drive shock front can cause significant shock propagation variations in Cu-doped Be, polyimide, and Ge-doped CH ablator samples. An accurate understanding of the ablator preheat will be essential for successful ignition of an indirect-drive ICF capsule at the NIF.

We thank S. Evans, J. Faulkner, and K. Lash for the setup and operation of the SOP. The $Be_{991}Cu_9$ samples were fabricated by G. Rivera and were characterized by R. Sebring. The Ge-doped CH samples were fabricated and characterized by A. Nikroo and J. Kaae of General Atomics. Sandia is a multiprogram laboratory operated by the Sandia Corporation, a Lockheed Martin Company, for the U.S. Department of Energy under Contract No. DE-AC04-94AL85000.

[1] J. D. Kilkenny *et al.*, Laser Part. Beams **17**, 159 (1999).
[2] P.-A. Holstein *et al.*, C. R. Acad. Sci., Ser. IV **1**, 693 (2000).
[3] R. E. Olson, Fusion Technol. **38**, 6 (2000).
[4] D. H. Munro *et al.*, Phys. Plasmas **8**, 2245 (2001).
[5] S. W. Haan *et al.*, Phys. Plasmas **2**, 2480 (1995).
[6] D. C. Wilson *et al.*, Fusion Technol. **38**, 16 (2000).
[7] R. E. Olson *et al.*, Phys. Plasmas **4**, 1818 (1997).
[8] R. W. Margevicius *et al.*, Fusion Technol. **35**, 106 (1999).
[9] T. R. Dittrich *et al.*, Fusion Technol. **31**, 402 (1997).
[10] C. Roberts *et al.*, Fusion Technol. **38**, 94 (2000).
[11] S. W. Haan *et al.*, Fusion Technol. **41**, 164 (2002).
[12] D. C. Wilson *et al.*, Phys. Plasmas **5**, 1953 (1998).
[13] R. E. Olson *et al.* (to be published).
[14] J. M. Soures *et al.*, Phys. Plasmas **3**, 2108 (1996).
[15] J. A. Oertel *et al.*, Rev. Sci. Instrum. **70**, 803 (1999).
[16] D. K. Bradley *et al.*, Rev. Sci. Instrum. **66**, 716 (1995).
[17] H. N. Kornblum, R. L. Kauffman, and J. A. Smith, Rev. Sci. Instrum. **57**, 2179 (1986).
[18] R. E. Turner *et al.*, Rev. Sci. Instrum. **70**, 656 (1999).
[19] A. Nobile *et al.*, Fusion Technol. (to be published).
[20] R. L. Kauffman *et al.*, Rev. Sci. Instrum. **66**, 678 (1995).
[21] G. B. Zimmerman and W. L. Kruer, Comments Plasma Phys. Controlled Fusion **2**, 51 (1975).
[22] Y. B. Zel'dovich and Y. P. Raizer, *Physics of Shock Waves and High Temperature Hydrodynamic Phenomena* (Academic Press, New York, 1966), p. 55.
[23] "Handbook of Material Properties Data Bases," edited by K. S. Holian, Los Alamos National Laboratory Report No. LA-10160-MS, 1984.
[24] J. F. Barnes, Phys. Rev. **153**, 269 (1967).
[25] L. J. Suter *et al.*, Phys. Plasmas **7**, 2092 (2000).